# Highly Efficient Targeted Mutagenesis in Mice Using TALENs

**Sudeepta Kumar Panda,*,†,[1] Benedikt Wefers,*,[1] Oskar Ortiz,* Thomas Floss,* Bettina Schmid,‡,§ Christian Haass,‡,§ Wolfgang Wurst,*,†,‡,** and Ralf Kühn*,†,[2]**

*Institute of Developmental Genetics, Helmholtz Zentrum München, German Research Center for Environmental Health, 85764 Munich, Germany, †Technische Universität München, 85350 Freising-Weihenstephan, Germany, ‡Deutsches Zentrum für Neurodegenerative Erkrankungen e. V., 80336 Munich, Germany, §Biochemistry and Munich Cluster for Systems Neurology, Adolf Butenandt Institute, Ludwig Maximilians University, 80336 Munich, Germany, and **Max-Planck-Institute of Psychiatry, 80804 Munich, Germany

**ABSTRACT** Targeted mouse mutants are instrumental for the analysis of gene function in health and disease. We recently provided proof-of-principle for the fast-track mutagenesis of the mouse genome, using transcription activator-like effector nucleases (TALENs) in one-cell embryos. Here we report a routine procedure for the efficient production of disease-related knockin and knockout mutants, using improved TALEN mRNAs that include a plasmid-coded poly(A) tail (TALEN-95A), circumventing the problematic *in vitro* polyadenylation step. To knock out the *C9orf72* gene as a model of frontotemporal lobar degeneration, TALEN-95A mutagenesis induced sequence deletions in 41% of pups derived from microinjected embryos. Using TALENs together with mutagenic oligodeoxynucleotides, we introduced amyotrophic lateral sclerosis patient-derived missense mutations in the fused in sarcoma (*Fus*) gene at a rate of 6.8%. For the simple identification of TALEN-induced mutants and their progeny we validate high-resolution melt analysis (HRMA) of PCR products as a sensitive and universal genotyping tool. Furthermore, HRMA of off-target sites in mutant founder mice revealed no evidence for undesired TALEN-mediated processing of related genomic sequences. The combination of TALEN-95A mRNAs for enhanced mutagenesis and of HRMA for simplified genotyping enables the accelerated, routine production of new mouse models for the study of genetic disease mechanisms.

GENETIC engineering of cells and organisms to create targeted mutants is a key technology for genetics and biotechnology. The ascent of the mouse as a mammalian genetic model is based on gene targeting through homologous recombination (HR) in embryonic stem (ES) cells (Capecchi 2005). Classical gene targeting via ES cells is a time- and labor-intense procedure that proceeds in the steps of vector construction, ES cell mutagenesis, chimera generation, and the transmission of mutant alleles through the germline (Hasty *et al.* 2000). Since the frequency of spontaneous HR in ES cells is low, it was a key finding that double-strand breaks (DSBs), created by sequence-specific nucleases, enhance local DNA repair by several orders of magnitude (Rouet *et al.* 1994). DSBs may be repaired through HR, using the sister chromosome as template or using gene targeting vectors that provide sequence homology regions flanking a desired genetic modification (Court *et al.* 2002; San Filippo *et al.* 2008). Alternatively, DSBs can be sealed by the nonhomologous end-joining (NHEJ) pathway that religates open ends without a repair template (Lieber 2010). By this means the DNA ends are frequently edited through the loss of multiple nucleotides, causing frameshift (knockout) mutations within coding regions. Targeted DSBs were first induced by zinc-finger nuclease (ZFN) fusion proteins that combine a DNA-binding domain made of zinc-finger motifs with the nuclease domain of *Fok*I (Porteus and Carroll 2005). The application of ZFNs in one-cell embryos provided proof-of-principle for the direct mutagenesis of the mouse, rat, and rabbit genome in a single step (Geurts *et al.* 2009; Carbery *et al.* 2010; Meyer *et al.* 2010; Flisikowska *et al.* 2011). Nevertheless, ZFNs do not provide a universal tool since the available code for the recognition


doi: 10.1534/genetics.113.156570
Manuscript received June 9, 2013; accepted for publication August 19, 2013
Supporting information is available online at http://www.genetics.org/lookup/suppl/doi:10.1534/genetics.113.156570/-/DC1.
[1]These authors contributed equally to this work.
[2]Corresponding author: Institute of Developmental Genetics, Helmholtz Zentrum München, German Research Center for Environmental Health, Ingolstaedter Landstr. 1, 85764 Munich, Germany. E-Mail: ralf.kuehn@helmholtz-muenchen.de

of nucleotide triplets is incomplete and multiple elements cannot be combined in a simple modular fashion. In contrast, the DNA-binding code of the transcription activator-like (TAL) proteins of *Xanthomonas* is based on the recognition of single nucleotides by individual peptide motifs, such that combinations of just four basic modules can be combined into domains that bind any target sequence (Boch *et al.* 2009; Moscou and Bogdanove 2009). Based on extensive experience with ZFNs, the TAL system could be readily adapted for gene editing by the fusion of DNA-binding modules with *Fok*I into TAL effector nucleases (TALENs) (Cermak *et al.* 2011; Miller *et al.* 2011). Taking advantage of its modular nature, a variety of cloning protocols enable us to assemble TALEN coding regions within a short time (Cermak *et al.* 2011; Reyon *et al.* 2012).

We recently reported that TALEN target sites are distributed in the mouse genome at an average spacing of 14 bp, enabling genome-wide targeted mutagenesis at high precision. In particular, we provided proof-of-principle that TALENs and oligodeoxynucleotides (ODNs) can be applied in one-cell embryos to introduce targeted mutations (Wefers *et al.* 2013). For HR- and NHEJ-mediated gene modifications, we achieved rates of 2% and 6%, respectively, using experimental conditions that were not yet optimized. Higher rates of NHEJ-mediated nucleotide deletions (>40%) were obtained upon the microinjection of TALEN mRNAs into the cytoplasm of one-cell embryos, tolerating larger injection volumes (Sung *et al.* 2013). Nevertheless, for the creation of targeted mutations it is instrumental to deliver DNA templates for HR together with TALEN mRNAs directly into the pronucleus, tolerating only minimal injection volumes. To set up an efficient routine procedure for mutagenesis we enhanced the activity of TALEN mRNAs to optimize nuclease expression upon pronuclear delivery, such that one or more knockin or knockout alleles are obtained among a group of mice derived from a single microinjection experiment. Upon the establishment of a mutant by embryo manipulation, the genotyping of breeding colonies imposes a constant workload. PCR-based protocols for the detection of subtle mutations often require the digestion of PCR products and gel electrophoresis. To minimize these efforts we validated whether high-resolution melt analysis (HRMA) represents a reliable and simplified tool for the genotyping of mouse mutants. HRMA identifies mutant PCR products by their specific denaturation profile (Liew *et al.* 2004) and requires no restriction digestion and size separation of PCR products.

We applied this streamlined procedure to introduce targeted and knockout mutations into the *Fus* and *C9orf72* genes to create disease models for inherited amyotrophic lateral sclerosis (ALS) and frontotemporal lobar degeneration (FTLD). Mutations disrupting the C-terminal nuclear localization sequence (NLS) of *FUS* have been identified in ALS patients (Kwiatkowski *et al.* 2009), whereas a hexanucleotide repeat expansion in the first intron of the *C9orf72* gene was found in patients representing ALS, FTLD, or both diseases (DeJesus-Hernandez *et al.* 2011; Renton *et al.* 2011). In the *Fus* gene dominant mutations within the NLS disrupt the nuclear import of FUS and lead to its cytoplasmic deposition in the brain and spinal cord of patients (Bosco *et al.* 2010; Gal *et al.* 2011; Ito *et al.* 2011; Kino *et al.* 2011; Dormann and Haass 2013). This defect is a key to pathogenesis since mutations that severely impair nuclear import, such as the P525L replacement, lead to an early onset and rapid progression of the disease. Since FUS is involved in multiple steps of gene expression, including transcription, pre-mRNA splicing, and mRNA transport, neurodegeneration may be caused by the loss of essential nuclear functions and/or the gain of a toxic function in the cytosol. Depletion of FUS in zebrafish and fruit flies causes a motoneuron phenotype but is perinatal lethal in mice (Hicks *et al.* 2000; Kabashi *et al.* 2011; Sasayama *et al.* 2012). To faithfully mimic the human codon replacements R521G and P525L, we targeted the analogous positions R513 and P517 of the mouse *Fus* gene, using TALENs and ODNs. As a cause of *C9orf72*-associated pathogenesis, the intronic repeat expansion may be deleterious through RNA-mediated toxicity or by the translation of repeat sequences, causing the production and aggregation of dipeptide repeat proteins (Ash *et al.* 2013; Mori *et al.* 2013) or both (Taylor 2013). To clarify whether *C9orf72* loss-of-function also contributes to the FTLD phenotype and to decipher its cellular function, we disrupted the mouse homolog of the *C9orf72* gene, *3110043O21Rik*, by the creation of TALEN-induced frameshift mutations.

Using our advanced TALEN mutagenesis procedure we obtained recombined *Fus* alleles in 6.8% and nucleotide deletions within *C9orf72* in 41% of mice derived from pronuclear embryo injections, validating this approach for the expedited recapitulation of disease-associated alleles. The established *Fus* codon replacement and *C9orf72* knockout mutants will be instrumental to studying genetic ALS and FTLD disease mechanisms.

## Materials and Methods

### *TALEN target sites*

For the selection of TALEN target sequences we used the "TALEN*designer*" (www.talen-design.de) as described in Wefers *et al.* (2013). Selected target sites cover two recognition sequences of 15 bp preceded by a T, separated by a spacer of 14–15 bp. To minimize off-target recognition, potential sites were analyzed using the "Paired Target Finder" (https://tale-nt.cac.cornell.edu) (settings: spacer length 13–20 bp, cutoff 3.0) (Doyle *et al.* 2012).

### *TALEN construction and expression*

Details on the construction of TALEN coding regions, expression vectors, and TALEN sequences are given in Supporting Information, File S1. For the expression of TALENs in mammalian cells we used the expression vector pCAG-TALEN-pA as described in Wefers *et al.* (2013). pT7-TALEN-95A was derived from pCAG-TALEN-pA by replacement

of the poly(A) signal sequence with a segment of 95 adenine residues derived from a mouse *Oct4* cDNA clone.

### *Oligodeoxynucleotides*

The oligodeoxynucleotides $ODN^{R513G}$ (5′-TGGGTAGGG TAGTTCAGTAACACGTAATCTAACATAACTTTTTCTTTCAG GGGCGAGCACAGACAGGAT**G**GCAGGGAGAGACCATATTAG CCTGGCTCCTGAAGTTCTGGAACTCTTCCTGTACCCAGTGT TACCCTTGT-3′) and $ODN^{P517L}$ (5′- TCAGTAACACGTAATC TAACATAACTTTTTCTTTCAGGGGCGAGCACAGACAGGATC GCAGGGAGAG**A**CTATATTAGCCTGGCTCCTGAAGTTCTGG AACTCTTCCTGTACCCAGTGTTACCCTTGTTATTTTGTAA ACT-3′) were synthesized and HPLC purified by Metabion (Martinsried, Germany), each having a length of 140 nt, including the targeted mutation (shown in boldface type) and a silent replacement (underlined), covering 70 bp upstream and downstream of the targeted codon.

### *Microinjection of one-cell embryos*

The injection of TALEN mRNA and targeting molecules (ODNs) was performed as described in Wefers *et al.* (2012, 2013), except that injections were done only into pronuclei. Briefly, capped TALEN mRNA was prepared in a single step by *in vitro* transcription from pT7-TALEN-95A plasmid DNA linearized with *Xba*I and *Ale*I (New England Biolabs, Frankfurt, Germany), using the mMessage mMachine T7 Ultra kit (omitting the polyadenylation step) and the MEGAclear kit (Life Technologies, Carlsbad, CA). The quality of synthesized mRNAs was controlled by agarose gel electrophoresis under denaturing conditions, using the NorthernMax-Gly system and the RNA Millenium size marker (Life Technologies). Each TALEN mRNA was then diluted in injection buffer (10 mM Tris, 0.1 mM EDTA, pH 7.2) to a working concentration of 90 ng/μl TALEN-Rik2 mRNA or 20 ng/μl TALEN-Fus15 mRNA. The targeting oligodeoxynucleotides were dissolved in water and diluted with injection buffer to a working concentration of 15 ng/μl. For microinjections, one-cell embryos were obtained by mating of (DBA/2 × C57BL/6)$F_1$ males with superovulated FVB/N females (Charles River, Sulzbach, Germany). One-cell embryos were injected with either only TALEN-Rik2 mRNA or a mixture of TALEN-Fus15 mRNA and the targeting oligodeoxynucleotides (15 ng/μl) ($ODN^{R513G}$ and $ODN^{P517L}$) into the larger pronucleus, but not into the cytoplasm. Test experiments showed that microinjections of Venus mRNA (90 ng/μl), using pronuclear capillaries, led to green fluorescence in all embryos, but the direct delivery of the same volume into the cytoplasm is less effective and labels only ∼10% of embryos. Injected zygotes were transferred into pseudopregnant CD1 female mice to obtain live pups. All mice showed normal development and appeared healthy. Mice were handled according to institutional guidelines approved by the animal welfare and use committee of the government of Upper Bavaria and housed in standard cages in a specific pathogen-free facility on a 12-h light/dark cycle with *ad libitum* access to food and water.

### *Isolation of genomic DNA*

Genomic DNA was isolated from tail tips of founder mice and their progeny, using the Wizard Genomic DNA Purification Kit (Promega, Mannheim, Germany), following the manufacturer's instructions.

### *HRMA*

For the screening of TALEN-induced mutations, the TALEN target regions of *C9orf72* and *Fus* (amplicon size 140 and 133 bp, respectively) were amplified in a 10-μl PCR reaction containing 40 ng lyophilized genomic DNA, 1 μl LC Green Plus+ Dye (Bioké, Leiden, The Netherlands), 200 nM of each dNTP, 250 nM each forward and reverse primers (Table S3), and 0.2 μl Phire Hot Start II DNA Polymerase (Thermo Scientific, Dreieich, Germany). PCR reaction protocols for mutagenic detection were 98°, 30 sec; 40 cycles of [98°, 5 sec; 62° (*C9orf72)*/66° (*Fus*), 5 sec; 72°, 5 sec]; 72°, 1 min; denaturation at 98°, 1 min; and rapid cool down to 25° for heteroduplex formation. Following the PCR, samples were analyzed with a LightScanner (BioFire Diagnostics, Salt Lake City) over a 65°–95° range. PCR products that contained mutant alleles were purified using the Qiaquick PCR purification kit (QIAGEN, Hilden, Germany), subcloned using the StrataClone Blunt PCR Cloning Kit (Agilent, Waldbronn, Germany), and sequenced (GATC Biotech, Konstanz, Germany). Sequences were compared to wild type, using the Vector NTI Advance 11.5 software suite (Life Technologies). To determine the detection limit of HRMA, cloned mutant PCR products from *C9orf72* founders R5 and R12 were diluted with wild-type PCR product. The melting curves of three replicates of each test sample were analyzed and compared to wild-type controls, using the LightScanner software with Call-IT 2.0 (BioFire Diagnostics).

### *Off-target analysis*

To assess potential TALEN off-target activity, the five highest-scored off-target sites (Table S2) were analyzed by HRMA in duplicate reactions, using locus-specific PCR primer pairs (see Table S3: *Fus* OS1–OS5 and Rik OS1–OS5). Four *Fus* and two *C9orf72* founders were compared to a C57BL/6 wild-type control. Founder-derived PCR products amplified from the *Fus* off-sites 1 and 3 were subcloned and sequenced. These sequences were compared to the respective genomic sequences of the C57BL/6, DBA/2, and FVB/N mouse strains (Ensembl Resequencing database, http://www.ensembl.org, release 71, April 2013).

## Results

### *Optimized expression of TALENs in one-cell mouse embryos*

To target the *Fus* and the *C9orf72* genes, we constructed TALEN pairs recognizing sequences within exon 15 and exon 2, respectively, using our TALEN*designer* algorithm and modular construction protocol (Wefers *et al.* 2013). The TALEN

coding regions were inserted into the mammalian expression vector pCAG-TALEN-pA, providing a CAG promoter and a polyadenylation signal sequence (Figure 1A). For the assessment of TALEN activity, expression vectors were cotransfected with customized nuclease reporter plasmids into HEK 293 cells as described in Wefers *et al.* (2013) and found to exhibit specific nuclease activity (Figure S1). For the expression of TALENs in one-cell embryos, the coding regions can be transcribed *in vitro* by T7 polymerase from linearized pCAG-TALEN-pA plasmids, followed by the polyadenylation of the coding RNA with poly(A) polymerase. Using this two-step protocol, we frequently noted an inconsistent production of single-species TALEN mRNAs, resulting in a smeared appearance of transcripts upon the polyadenylation step [Figure 1C, TALEN-poly (A)]. This effect occurred for TALEN but not for shorter, *e.g.*, ZFN RNAs, possibly because the transcription of the 3-kb TALEN coding region leads to a larger fraction of truncated products, contaminating the polyadenylation reaction. To enable the reliable production of TALEN mRNAs, for optimal nuclease expression upon pronuclear injection, we inserted the TALEN coding regions into pT7-95A (Figure 1B). This vector provides a T7 promoter and a region of 95 adenine (A) residues located downstream of the TALEN coding region for the production of polyadenylated (TALEN-95A) mRNAs in a single step. Using pT7-TALEN-95A vectors for *in vitro* transcription, we reproducibly obtain full-length TALEN mRNAs of the expected size of 2948 nucleotides (Figure 1C, TALEN-95A). To determine the RNA concentration that supports efficient translation upon pronuclear microinjection, we used a 95A RNA encoding the Venus reporter. We found green fluorescence in all embryos microinjected with Venus-95A RNA at 90 ng/μl, upon culture to the two-cell stage (Figure 1D). To assess the potency of TALEN-95A RNAs for the mutagenesis of the *C9orf72* and *Fus* genes we used concentrations of 90 ng/μl and 20 ng/μl, respectively.

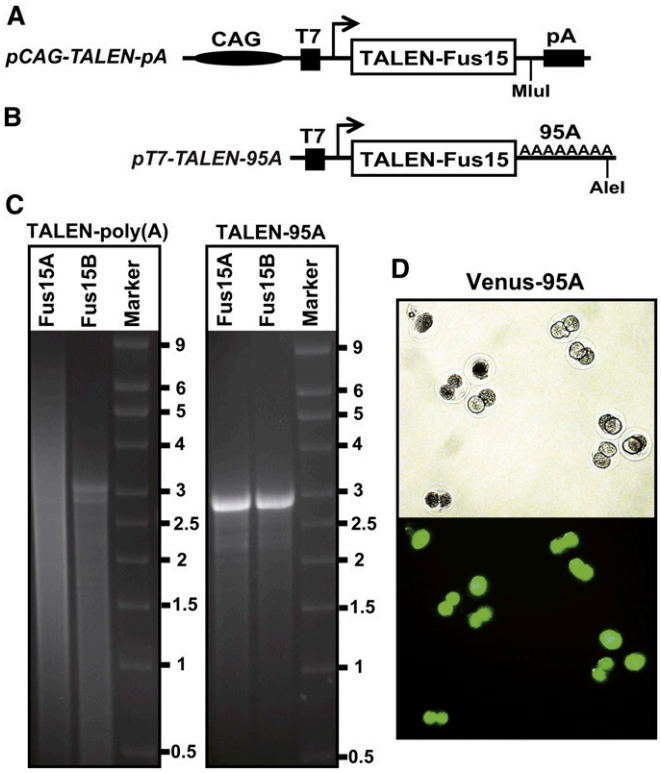


**Figure 1** Production of TALEN mRNAs for embryo microinjection. (A) Plasmid pCAG-TALEN-Fus15-pA provides a CAG promoter (CAG) and a poly(A) signal sequence (pA) for expression of TALEN-Fus15 proteins in mammalian cells. TALEN mRNA can be produced *in vitro* from *Mlu*I-linearized plasmid DNA in a two-step procedure, using T7 polymerase for transcription and poly(A) polymerase for polyadenylation. (B) Plasmid pT7-TALEN-Fus15-95A provides a T7 promoter (T7) and a region of 95 adenine (95A) nucleotides, followed by an *Ale*I site. TALEN RNA, including a plasmid-coded poly(A) sequence, can be produced in a single step, using T7 polymerase and *Ale*I-linearized plasmid DNA. T7: T7 promoter region. (C) Agarose gel electrophoresis of reaction products transcribed with T7 polymerase from *Mlu*I-linearized pCAG-TALEN-Fus15-pA plasmids, followed by polyadenylation with poly(A) polymerase [left gel, TALEN-poly(A)], or produced in a single step with T7 polymerase from *Ale*I-linearized pT7-TALEN-Fus15-95A plasmids (right gel, TALEN-95A). The size of full-length TALEN-95A transcripts is expected at 2948 nt. Marker: RNA size marker (×1000 nucleotides). (D) Microinjection of *in vitro*-produced Venus-95A RNA (90 ng/μl) into pronuclei of one-cell mouse embryos. The manipulated embryos were cultured to the two-cell stage and analyzed for Venus expression by fluorescence microscopy. Top, white light; bottom, green fluorescence.

### *Generation of C9orf72 knockout mice*

To induce frameshift mutations within the mouse homolog of *C9orf72* we designed a TALEN pair (TALEN-Rik2) targeting a sequence downstream of the start codon located within the second exon of the murine *3110043O21Rik* gene (Figure 2A and Figure 3, A and C).

From pronuclear microinjections of TALEN-Rik2 mRNAs (95A type, 90 ng/ul), we obtained 51 pups (Table 1) that were screened for the presence of mutant alleles by HRMA of PCR products covering the targeted exon. Twenty-one of these mice (41%) were identified as founders harboring mutant *C9orf72* alleles, confirming that the pronuclear delivery of 95A-type mRNAs leads to a high mutagenesis rate. Representative HRMA results from 8 founders are shown in Figure 2 and Figure S2, exhibiting melting curves that deviate from the wild-type control. We selected 11 founders for the further characterization of modified *C9orf72* alleles by subcloning and sequence analysis of PCR products. Among founders R5–R32 we identified 12 mutant alleles (Figure 3A) that exhibit deletions of 1–36 nucleotides or a 2-bp insertion within the TALEN target region. Seven of these deletions disrupt the *C9orf72* reading frame in between codons 6–9 and are predicted for the translation of 8–11 additional amino acids (Figure 3B). For the establishment of a mutant breeding colony, founder R23 was mated to wild-type mice and its progeny genotyped by PCR and HRMA. Seven of 15 pups derived from R23 showed melting curves distinguished from the wild-type control and the sequencing of PCR products from pup R23-15 confirmed the germline transmission of the parental *C9orf72* allele (Figure 3C).

Founders obtained from microinjections of TALENs or ZFNs are frequently mosaics, harboring a mutation only in

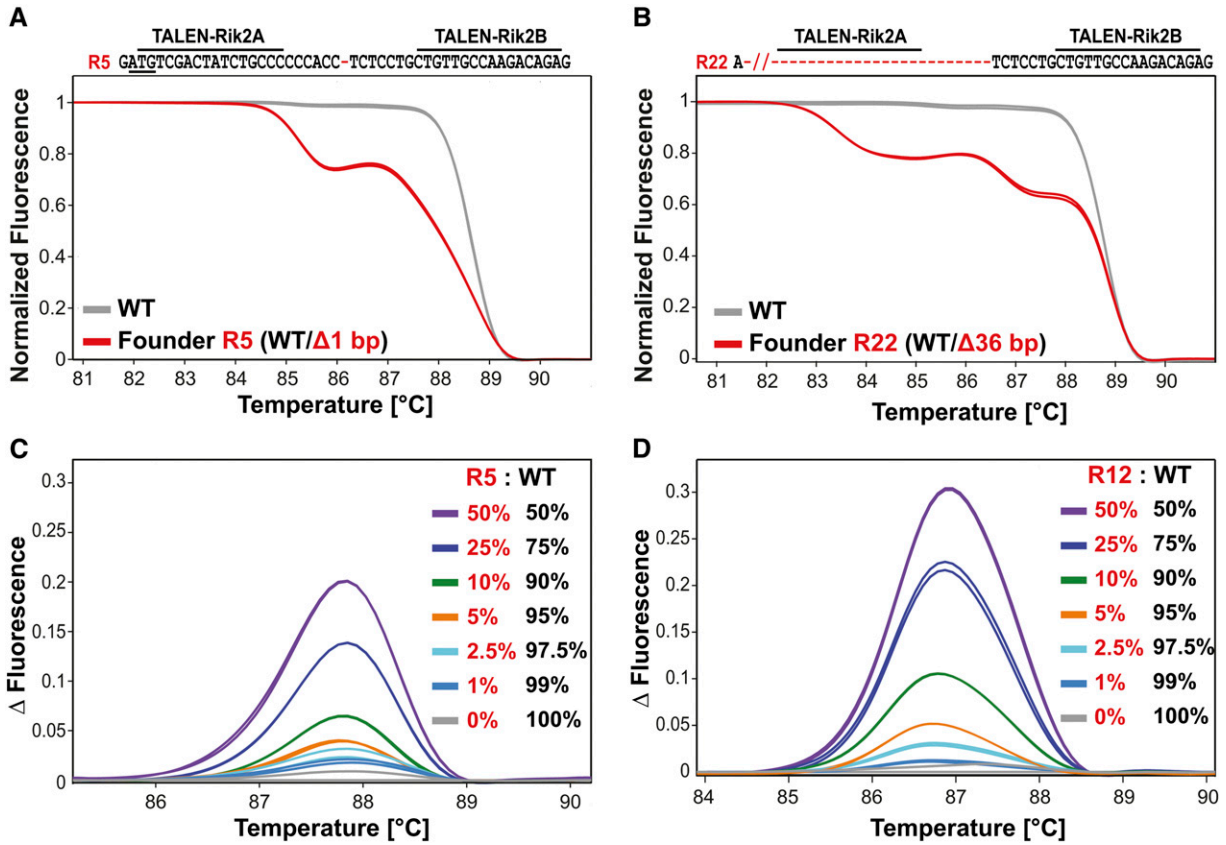


**Figure 2** Identification of *C9orf72* mutants by HRMA. (A and B) Melting analysis of PCR products amplified in duplicate from tail DNA of founder R5 (A) and of founder R22 (B) (red curves, overlaid) in comparison to wild-type controls (gray curves, overlaid). The TALEN-Rik2 target sequences within exon 2 are shown (start codon underlined); nucleotides deleted in mutant alleles are shown as red dashes and genotypes are given in parentheses. (C and D) The sensitivity of HRMA for mutant detection was determined by analyzing HRMA samples prepared with varying amounts of wild-type or mutant PCR products from founder R5 (1-bp deletion, C) and founder R12 (6-bp deletion, D). The limit to detect the R5 allele is at 5% for the mutant product (orange curve) and at 2.5% for the R12 allele (light blue curve).

some of the somatic cells, if gene editing occurred after genome replication (Wefers *et al.* 2013). To assess whether mosaic mutant genotypes can be identified by HRMA, we performed control experiments to establish its detection limits. For this purpose we prepared HRMA test samples containing 1–50% of cloned, mutant *C9orf72* PCR product (allele R5, 1-bp deletion; or R12, 6-bp deletion) and 99–50% of wild-type PCR product. In comparison to the wild-type controls, the presence of mutant alleles could be reliably detected in samples containing 5% (1-bp deletion) or 2.5% (6-bp deletion) of mutant DNA (Figure 2, C and D). These results indicate that mosaic founders harboring even a minor fraction of mutant cells can be recognized by melting analysis and validate HRMA as a simple and sensitive tool for the identification of mutants derived from embryo microinjection of TALENs.

### *Generation of Fus$^{R513G}$ and Fus$^{P517L}$ codon replacement mutants*

To recapitulate the patient-derived codon replacements R521G and P525L in the mouse *Fus* gene, we targeted the analogous positions R513 and P517, using synthetic oligodeoxynucleotides as template for TALEN-induced HR. We designed a TALEN pair (TALEN-Fus15) recognizing the C-terminal coding sequence located within exon 15 (Figure 4A). The oligonucleotides ODN$^{R513G}$ and ODN$^{P517L}$ cover 140 nt centered on exon 15 and include nucleotide replacements that redefine the codons 513 and 517 into glycine (R513G) or leucine (P517L), respectively. To exclude the potential reprocessing of recombined alleles by TALENs, each ODN included an additional, silent nucleotide replacement within the TALEN-Fus15B recognition sequence. TALEN-Fus15 mRNAs (95A type, 20 ng/μl) were co-injected with ODN$^{R513G}$ or ODN$^{P517L}$ into the pronuclei of one-cell embryos. We obtained 83 pups from the injections of ODN$^{R513G}$ and 50 pups from ODN$^{P517L}$ (Table 1), which were screened for mutations by HRMA of PCR products covering exon 15. The samples from 8 mice from ODN$^{R513G}$ (9.6%) and 2 mice from ODN$^{P517L}$ (4%) injections showed melting curves distinguished from the wild-type control (Figure S3) and were further analyzed by the subcloning and sequencing of each of the five PCR products. The founders derived from ODN$^{R513G}$ injections harbored 14 modified *Fus* alleles (Figure 4A). Four founders contained the desired R513G replacement together with (F69, F70) or without (F29, F37) the silent replacement within the TALEN-Fus15B binding region. Three

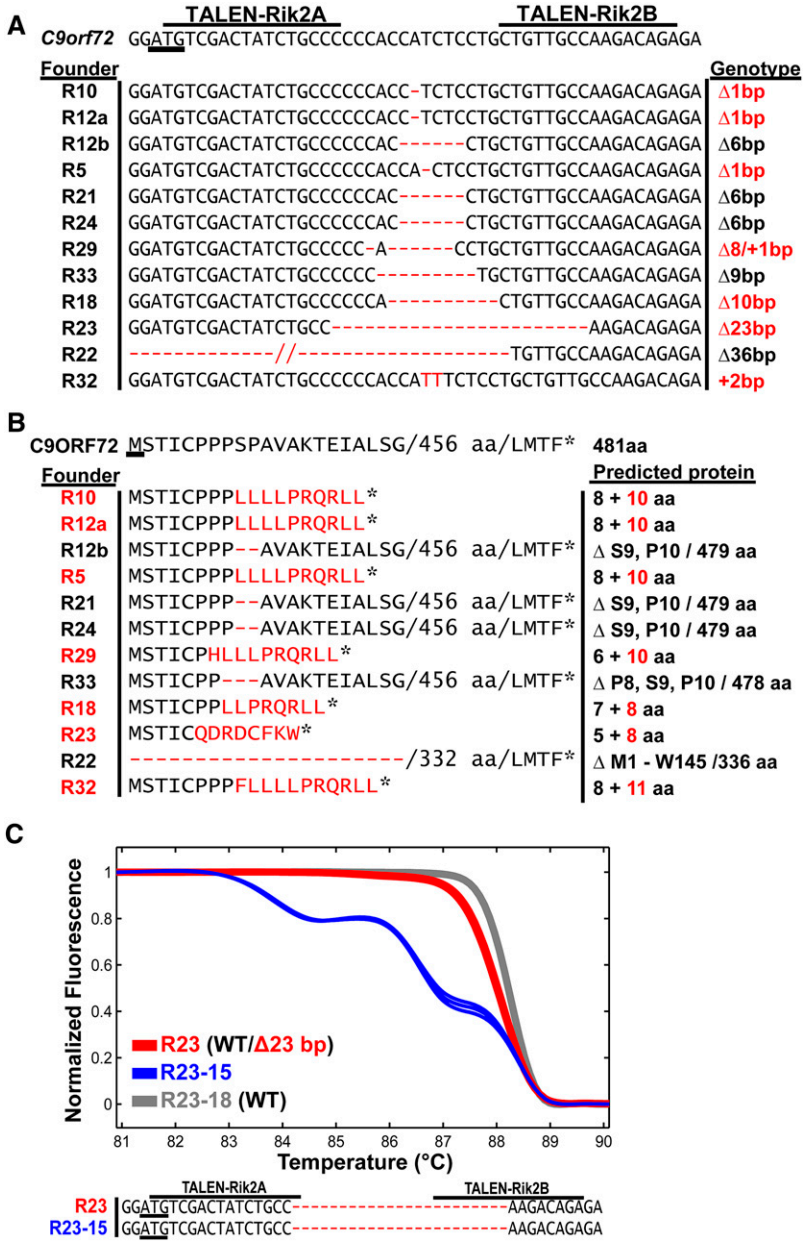


**Figure 3** TALEN-induced *C9orf72* alleles. (A) Sequence comparison of the TALEN-Rik2 target region within exon 2 of *C9orf72* in comparison to mutant alleles amplified by PCR from tail DNA of the indicated founders. The start codon of *C9orf72* is underlined and the recognition sequences of TALENs are indicated. Nucleotide deletions and insertions are shown as red dashes and red letters, respectively. The genotype classifies mutant alleles as products of NHEJ-associated deletion (Δ) or insertion (+); alleles exhibiting reading frameshifts are shown in red. Founder R12 contained two mutant alleles showing the deletion of 1 or 6 bp, respectively. (B) Predicted protein sequences of TALEN-induced *C9orf72* alleles (start codon underlined). Upon the translation of the first five to eight wild-type codons, the mutant alleles R10, R12a, R5, R29, R18, R23, and R32 exhibit a reading frameshift, followed by a nonsense sequence of 8–11 residues (red letters) and a stop codon (asterisk). Allele R22 lost the start codon (Δ ATG) and may result in the complete loss of translation or in translational initiation at the downstream ATG codon 146 and the production of a truncated protein. The alleles R12b, R21, R24, and R33 show only deletions of codons 8–10 or 9–10 and preserve the downstream reading frame of *C9orf72*. (C) Melting analysis of triplicate PCR products from founder R23 (red curves, overlaid), its pup R23-15 (blue curves), and a wild-type C57BL/6 control (gray curves). The sequence analysis of cloned PCR products confirmed the germline transmission of the R23 allele.

founders (F18, F75, and F79) showed recombined R513G *Fus* alleles that included unintended single-nucleotide alterations (Figure 4A), likely resulting from ODN synthesis errors. Indeed, we noted that our ODN$^{R513G}$ synthesis used for microinjection contained a substantial fraction (~1/3) of variant molecules, as determined by PCR, subcloning, and sequencing (data not shown). Furthermore, four of the founders harbored additional modified *Fus* alleles that underwent nucleotide deletions (F37b, F70b, F75d, and F5) or showed an unexpected nucleotide replacement within codon 512 (F69b). From the microinjection of ODN$^{P517L}$ both founders harbored recombined *Fus* alleles, including the P517L and adjacent silent replacements (F4, F36a, Figure 4B). Founder F36 was mosaic for another recombined allele, including a 14-bp deletion (F36b) and a deletion allele that lost 12 bp (F36c).

For the establishment of *Fus* mutant lines we mated founders F29 (*Fus*$^{R513G}$, Figure 4C) and F36 (*Fus*$^{P517L}$, Figure 4D) to wild-type mice and genotyped their offspring by PCR and HRMA. Eight of 15 pups derived from F29 and 8 of 12 pups from F36 showed melting curves differing from the wild-type control and the cloning and sequencing of PCR products confirmed the germline transmission of the parental *Fus*$^{R513G}$ (pup F29-24, Figure 4C) and *Fus*$^{P517L}$ alleles (pup F36-13, Figure 4D). Five additional founders were mated to wild-type mice and transmitted modified *Fus* loci to their offspring, as confirmed by HRMA (Table S1).

These results show that TALENs and ODNs created recombined *Fus* loci in 6.8% of mice derived from microinjections (1 recombined founder per 15 pups, Table 1) and that mutations identified in the founders' tail DNA were faithfully transmitted through the germline. To further confirm the

**Table 1 TALEN-mediated gene editing events**

| Microinjection experiment | TALEN mRNA concentration (ng/μl) | No. pups | No. mutant founders (%) | Founders' NHEJ events (%) | Founders' HR events (%) |
|---|---|---|---|---|---|
| 1. TALEN-Rik2 | 90 | 51 | 21 (41.2) | 21 (41.2) | — |
| 2. TALEN-Fus15 + ODN$^{R513G}$ | 20 | 83 | 8 (9.6) | 8 (9.6) | 7 (8.4) |
| 3. TALEN-Fus15 + ODN$^{P517L}$ | 20 | 50 | 2 (4) | 2 (4) | 2 (4) |
| TALEN-Fus15 $\sum$ = | | 133 | 10 (7.5) | 10 (7.5) | 9 (6.8) |

Shown are mutant founder mice and mutant alleles obtained from the microinjection of Rik TALENs or Fus TALENs together with mutagenic ODNs into the pronuclei of one-cell embryos. The concentration of TALEN mRNAs and the number of pups obtained from embryo transfers are shown. Within these groups the overall frequency of TALEN-induced gene editing is indicated by the number of mice harboring mutant alleles (mutant founders), modified either by NHEJ or by HR events. Half of the founders derived from experiments 2 and 3 were mosaics, containing more than one modified allele. Therefore, the combined number of mice exhibiting alleles modified by NHEJ or HR exceeds the total number of mutant founders.

integrity of the targeted *Fus$^{R513G}$* locus we amplified genomic sequences covering 3.4 kb upstream of codon 513 and 3.2 kb of the downstream region, using tail DNA of the heterozygous *Fus$^{R513G}$* pup F29-24. The direct sequencing of both PCR products, representing molecules derived from the wild type and the *Fus$^{R513G}$* allele, revealed a uniform reading pattern of the *Fus* wild-type sequence, except for the C to G replacement within codon 513 that showed a mixed G/C peak (Figure S5). This result proves the genomic integrity of the *Fus$^{R513G}$* allele within a region of 6.6 kb centered on codon 513. To further analyze the functionality and transcription of the *Fus$^{R513G}$* allele we isolated mRNA from the tail of pup F29-24, prepared *Fus* cDNA, and PCR amplified a 341-bp region of the *Fus* transcript covering exons 14 and 15. The sequence analysis of cloned PCR products revealed spliced cDNA sequences including the R513G replacement, confirming the functionality of the *Fus$^{R513G}$* allele (Figure S4).

### *Analysis of TALEN off-target activity*

TALENs may recognize genomic (off-target) sites, which are similar to the intended target sequence and cause undesired genetic modifications. To assess the frequency of such off-target events in mutants derived from TALEN microinjections, we analyzed for each pair of our TALENs five off-target sites (Table S2) (Doyle *et al.* 2012), using tail DNA from four *Fus* and two *C9orf72* founder mutants. PCR products covering these regions were analyzed by HRMA in comparison to a C57BL/6 wild-type control (Figure 5). Whereas the melting curves of all TALEN-Rik2 and of three TALEN-Fus15 off-target sites were identical to the controls, the PCR products from the *Fus* off-sites 1 and 3 were distinguished from the control. These PCR products were subcloned and the analysis of five sequences per sample revealed single-nucleotide substitutions that represent known polymorphisms in the genome of the inbred strains (Figure S6) we used for embryo production. Hence, we found no evidence for the presence of off-target mutations in founders derived from microinjections of our TALENs.

## Discussion

Single-nucleotide polymorphisms leading to codon replacements within human genes are increasingly identified as disease-related mutations by high-throughput genomic analysis such as exome sequencing. Genetic mouse models that recapitulate such mutations will be instrumental to studying the underlying disease mechanisms and to developing therapeutic interventions. We recently provided proof-of-principle that nucleotide and codon replacements can be directly introduced into the mouse genome by microinjection of TALEN mRNAs (15 ng/μl) and ODNs into the pronuclei of one-cell embryos (Wefers *et al.* 2013). For the *Rab38* locus we achieved a rate of 1.8% for targeted replacements and of 4.8% for NHEJ-mediated deletions, using as yet nonoptimized conditions. To enable the routine production of targeted mouse models at high efficiency, we aimed to enhance gene editing by increasing the incidence of TALEN-induced DSBs upon pronuclear delivery. High rates (>40%) of NHEJ-mediated deletions have been achieved by the microinjection of TALEN mRNAs into the embryonic cytoplasm (Sung *et al.* 2013), tolerating large volumes, but this route provides no option for the codelivery of DNA templates into the nucleus. Since pronuclei tolerate only minimal volumes and narrow injection capillaries, restricted for the delivery of a few picoliters, we sought to optimize the activity and concentration of the co-injected TALEN mRNAs. To this end we used mRNAs with template-coded poly(A) regions (95A) and found that pronuclear delivery at 90 ng/μl leads to the effective translation of a fluorescent reporter. As a validation of this protocol we found that deletions in *C9orf72* were induced in 41% of pups derived from injections of TALEN mRNAs at 90 ng/μl. For the targeting of *Fus* we used TALEN-95A mRNAs at a lower concentration (20 ng/μl) together with ODNs, comparable to the earlier targeting of *Rab38*, and found targeted replacements to occur at a rate of 6.8%. These rates of gene editing are four- to eightfold higher compared to our previous results from *Rab38*, suggesting that TALEN-95A mRNAs lead to enhanced mutagenesis. At these rates one or more targeted alleles can be obtained from a single day of microinjection, typically resulting in ~25 pups if FVB-derived embryos are used for microinjection. TALENs have been further used to induce knockout mutations in embryos of the C57BL/6 inbred strains upon cytoplasmic delivery (Davies *et al.* 2013; Sung *et al.* 2013; Qiu *et al.* 2013). Therefore we are confident that it will be also possible to generate targeted mutations by the delivery of TALEN-95A mRNAs and targeting DNA molecules into the pronuclei of C57BL/6 embryos. Nevertheless, the number of live births from C57BL/6 embryos is about half compared to

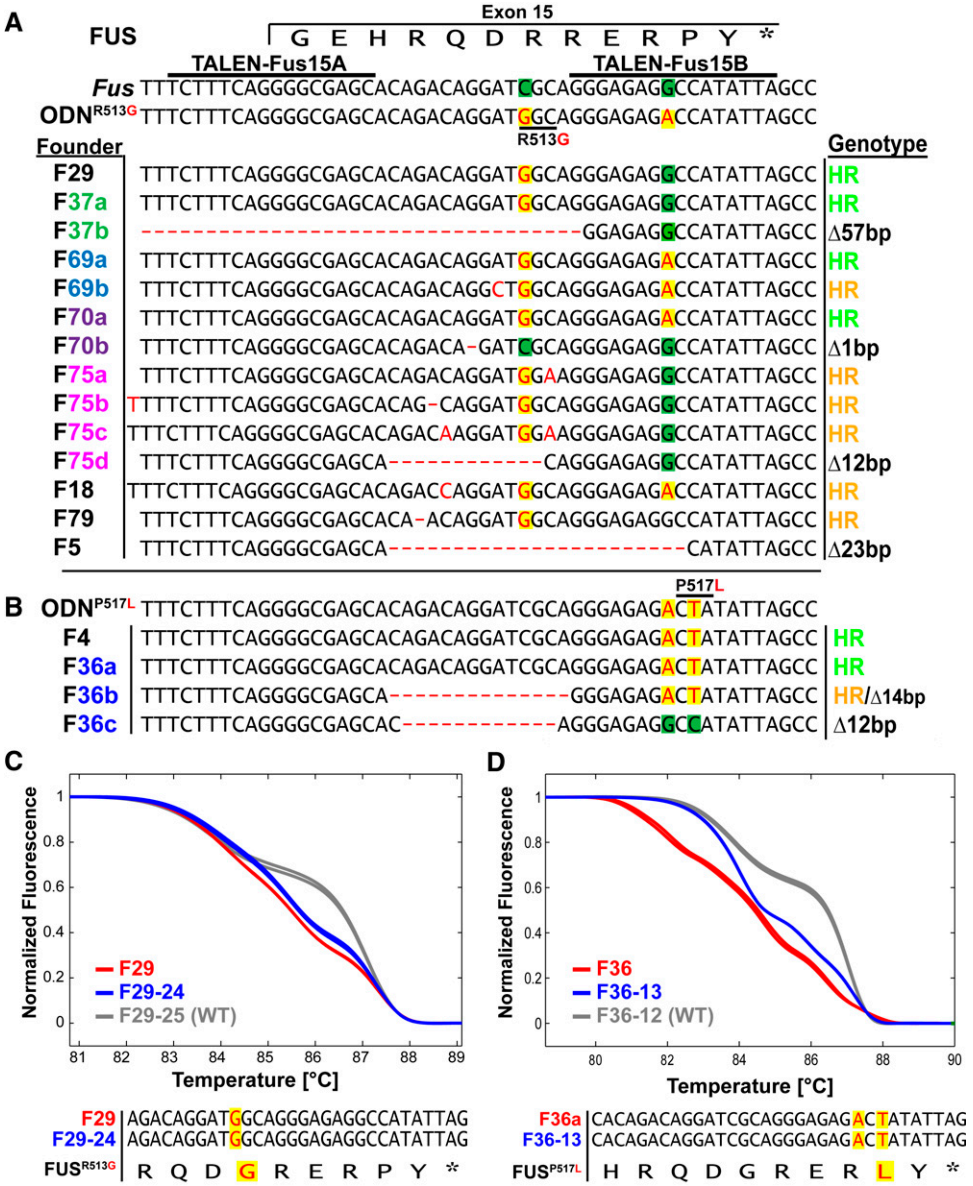


**Figure 4** Generation of *Fus*$^{R513G}$ and *Fus*$^{P517L}$ mutants. (A and B) Sequence comparison of the TALEN target region covering the *Fus* exon 15, of ODN$^{R513G}$, ODN$^{P517L}$, and cloned PCR products amplified from tail DNA of ODN$^{R513G}$ (A) and ODN$^{P517L}$ (B) founder mutants, identified by HRMA. The exon 15 coded FUS sequence, the TALEN binding sites, and codons 513 and 517 are indicated; nucleotides deviating from wild type (green background) are shown in red on a yellow background. Nucleotide deletions or insertions are shown as red dashes or red letters. The genotype describes the mutant alleles as a product of homologous recombination (HR) or NHEJ-associated deletion (Δ) or insertion (+). (C and D) Melting analysis of duplicate PCR products from founder F29 (ODN$^{R513G}$) (C) (red curves) its pup F29-24 (blue curves) and founder F36 (ODN$^{P517L}$) (D) (red curves) and its pup F36-13 in comparison to wild-type controls (gray curves). The sequence analysis of cloned PCR products from pups F29-24 and F36-13 confirmed the germline transmission of the *Fus*$^{R513G}$ and *Fus*$^{P517L}$ alleles.

that from the FVB strain such that 2 days of microinjection will be required to recover 25 pups.

Several *Fus* founders recombined with the 140-nt ODN$^{R513G}$ showed unintended nucleotide insertions, deletions, or replacements. These alterations likely result from the error-prone synthesis of oligonucleotides and identify ODN quality and length as important factors to optimize the net rate of correctly modified alleles. Since the synthesis of shorter ODNs correlates with an increased fraction of correct molecules, it will be of future interest to determine the *in vivo* recombination rate of ODNs in relation to the molecules' length. In mammalian cell lines it has been shown that a minimum of 50 bp of homology is sufficient to achieve a high recombination rate (Chen *et al.* 2011).

As previously observed for ZFN- and TALEN-induced mutagenesis, a part of our *Fus* and *C9orf72* founders were mosaic for one or more modified alleles, resulting from multiple, independent editing events that may occur before or after the first or second cycle of genome replication. Since modified loci are first identified in the founder's tail DNA, it is essential that the same alleles are present in the germ cell population to establish breeding colonies. Each of eight mated founders transmitted mutant alleles to 10–67% of its progeny, thereby confirming the contribution of mutant cells to the germline. Furthermore, the resequencing of *Fus* and *C9orf72* alleles from heterozygous pups confirmed the identity to the parental loci, indicating that the analysis of tail DNA is predictive of the mutational spectrum in the germline.

At present little is known about the potential processing of sites that are similar to the intended TALEN target sequence and which degree of sequence divergence is necessary to exclude off-target recognition. Using tail DNA from *Fus* and *C9orf72* founders we analyzed five potential off-target sites

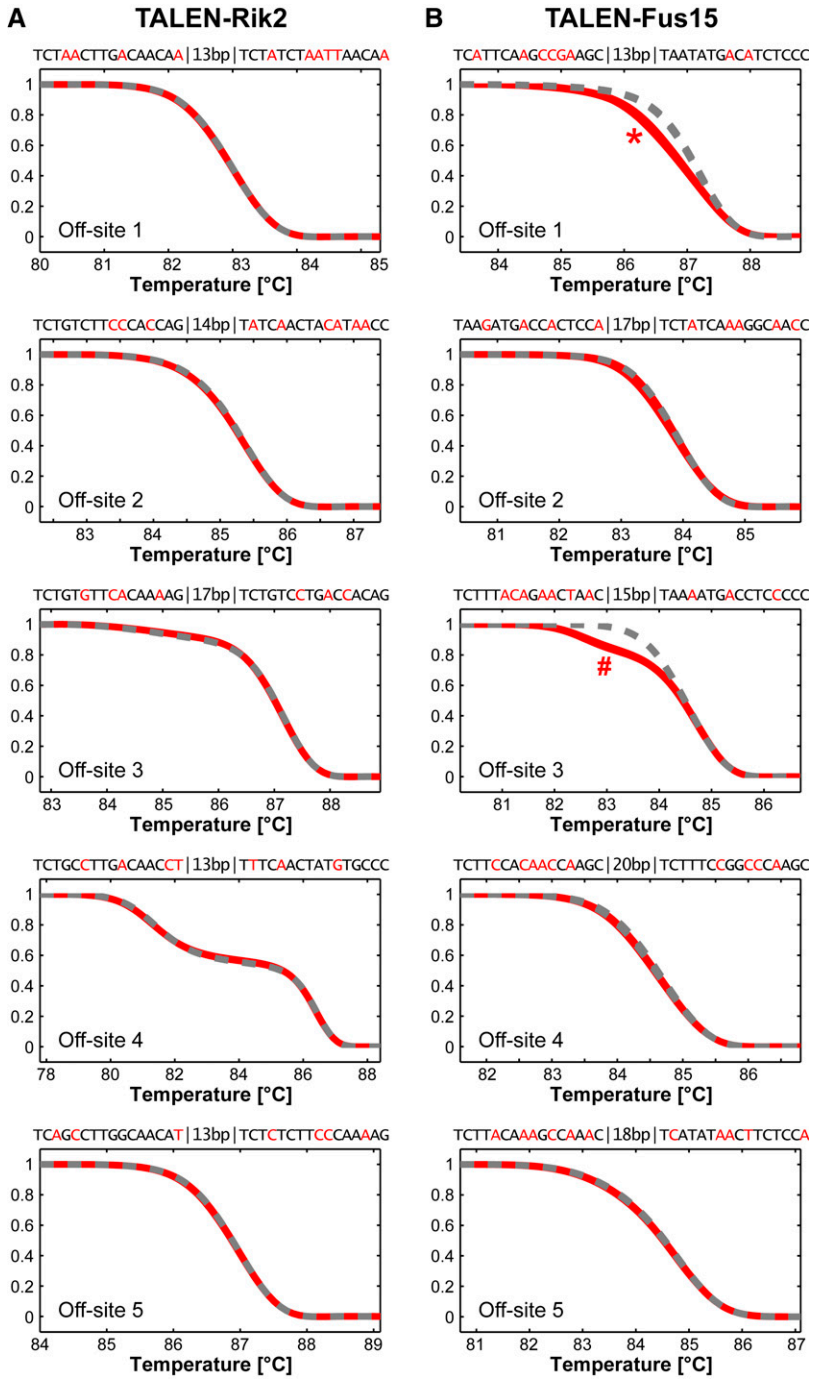


**Figure 5** Genome-wide off-target analysis of TALEN-Rik2 and TALEN-Fus15. (A and B) Melting analysis of predicted off-target sites of TALEN-Rik2 (A) and TALEN-Fus15 (B) in wild-type and mutant founder mice (R5, R23 and F5, F29, F4, F36). The potential TALEN target sequences, spacer length, and mismatches (red letters) to the *Fus* and *C9orf72* target sites are indicated. HRMA revealed no differences from the C57BL/6 wild-type control (dashed gray curves) and founder-derived PCR products (red curves), except for the *Fus*15 off sites 1 (*) and 3 (#), which were identified as polymorphisms present in the different genetic backgrounds. Details on these polymorphisms are shown in Figure S6.

by HRMA and found no indication for processing at these sites. Since for TALEN-Fus15 and Rik2 the closest genomic off sites are distinguished by seven or more nucleotide substitutions, our results suggest that under this condition TALENs do not cause modifications at sites that are predictable with the known binding code. Whether TALENs also recognize other, presently unpredictable target sites requires further clarification by whole-genome sequencing.

Besides the one-time generation of mutant alleles by embryo manipulation, the genotyping of mutant offspring adds a constant workload to the maintenance of breeding colonies. Mutant alleles harboring nucleotide replacements cannot be identified through the mere size of PCR products. Therefore, present PCR genotyping protocols require differentiating between wild-type and mutant alleles by digestion with restriction enzymes and gel electrophoresis. This rationale often requires the incorporation of additional, undesired nucleotide substitutions to create or delete enzyme recognition sites. All of these drawbacks are relieved by automated HRMA that requires just the melting analysis of PCR reactions. Our characterization of mutant *Fus* and *C9orf72* founders and their offspring validated HRMA as a universal

and sensitive tool for the identification and genotyping of TALEN-induced nucleotide replacements and deletions. By the inclusion of wild-type control DNA it will be further possible to differentiate heterozygous and homozygous mutant genotypes by HRMA.

Taken together, our advanced TALEN mutagenesis and analysis procedure enables the accelerated, routine production of new genetic mouse models. Since TALENs combined with ODNs allow genome-wide targeting at high precision, this technology supports expedited *in vivo* analysis of newly discovered disease-associated mutations.

## Acknowledgments

We thank R. Kneuttinger, P. Kunath, A. Krause, A. Tasdemir, S. Weidemann and O. Yefremova, for excellent technical assistance. This work was supported by the European Union within the European Conditional Mouse Mutagenesis (EUCOMM) project (LSHG-CT-2005-018931, to W.W.), by the German Ministry of Education and Research within the Disease Genes to Proteins (DIGTOP) project (01GS0858, to W.W. and R.K.) of the National Genome Research Network (NGFN)-Plus program, by the excellence cluster for systems neurology (SyNergy) 1010 (to. C.H., B.S., W.W.), by the Kompetenznetzwerk Degenerative Demenzen (KNDD2) (FKZ01GI1005D to T.F), and by the Indian Council of Agricultural Research (No.29-1/2009-EQR/Edn, to S.K.P.). The research leading to these results has received funding from the European Research Council under the European Union's Seventh Framework Programme (FP7/2007-2013)/ European Research Council grant agreement n°321366-Amyloid, to C.H.).

## Literature Cited

Ash, P. E. A., K. F. Bieniek, T. F. Gendron, T. Caulfield, W.-L. Lin *et al.*, 2013 Unconventional translation of C9ORF72 GGGGCC expansion generates insoluble polypeptides specific to c9FTD/ALS. Neuron 77: 639–646.

Boch, J., H. Scholze, S. Schornack, A. Landgraf, S. Hahn *et al.*, 2009 Breaking the code of DNA binding specificity of TAL-type III effectors. Science 326: 1509–1512.

Bosco, D. A., N. Lemay, H. K. Ko, H. Zhou, C. Burke *et al.*, 2010 Mutant FUS proteins that cause amyotrophic lateral sclerosis incorporate into stress granules. Hum. Mol. Genet. 19: 4160–4175.

Capecchi, M. R., 2005 Gene targeting in mice: Functional analysis of the mammalian genome for the twenty-first century. Nat. Rev. Genet. 6: 507–512.

Carbery, I. D., D. Ji, A. Harrington, V. Brown, E. J. Weinstein *et al.*, 2010 Targeted genome modification in mice using zinc-finger nucleases. Genetics 186: 451–459.

Cermak, T., E. L. Doyle, M. Christian, L. Wang, Y. Zhang *et al.*, 2011 Efficient design and assembly of custom TALEN and other TAL effector-based constructs for DNA targeting. Nucleic Acids Res. 39: e82.

Chen, F., S. M. Pruett-Miller, Y. Huang, M. Gjoka, K. Duda *et al.*, 2011 High-frequency genome editing using ssDNA oligonucleotides with zinc-finger nucleases. Nat. Methods 8: 753–755.

Court, D. L., J. A. Sawitzke, and L. C. Thomason, 2002 Genetic engineering using homologous recombination. Annu. Rev. Genet. 36: 361–388.

Davies, B., G. Davies, C. Preece, R. Puliyadi, D. Szumska *et al.*, 2013 Site specific mutation of the Zic2 locus by microinjection of TALEN mRNA in mouse CD1, C3H and C57BL/6J oocytes. PLoS ONE 8: e60216.

DeJesus-Hernandez, M., I. R. Mackenzie, B. F. Boeve, A. L. Boxer, M. Baker *et al.*, 2011 Expanded GGGGCC hexanucleotide repeat in noncoding region of C9ORF72 causes chromosome 9p-linked FTD and ALS. Neuron 72: 245–256.

Dormann, D., and C. Haass, 2013 Fused in sarcoma (FUS): an oncogene goes awry in neurodegeneration. Mol. Cell. Neurosci. DOI: 10.1016/j.mcn.2013.03.006.

Doyle, E. L., N. J. Booher, D. S. Standage, D. F. Voytas, V. P. Brendel *et al.*, 2012 TAL Effector-Nucleotide Targeter (TALE-NT) 2.0: tools for TAL effector design and target prediction. Nucleic Acids Res. 40: W117–W122.

Flisikowska, T., I. S. Thorey, S. Offner, F. Ros, V. Lifke *et al.*, 2011 Efficient immunoglobulin gene disruption and targeted replacement in rabbit using zinc finger nucleases. PLoS ONE 6: e21045.

Gal, J., J. Zhang, D. M. Kwinter, J. Zhai, H. Jia *et al.*, 2011 Nuclear localization sequence of FUS and induction of stress granules by ALS mutants. Neurobiol. Aging 32: 2323.e27–40.

Geurts, A. M., G. J. Cost, Y. Freyvert, B. Zeitler, J. C. Miller *et al.*, 2009 Knockout rats via embryo microinjection of zinc-finger nucleases. Science 325: 433.

Hasty, P., A. Abuin, and A. Bradley, 2000 Gene targeting, principles, and practice in mammalian cells, pp. 1–35 in *Gene Targeting: A Practical Approach*, *The Practical Approach Series*, edited by A. Joyner. Oxford University Press, Oxford.

Hicks, G. G., N. Singh, A. Nashabi, S. Mai, G. Bozek *et al.*, 2000 Fus deficiency in mice results in defective B-lymphocyte development and activation, high levels of chromosomal instability and perinatal death. Nat. Genet. 24: 175–179.

Ito, D., M. Seki, Y. Tsunoda, H. Uchiyama, and N. Suzuki, 2011 Nuclear transport impairment of amyotrophic lateral sclerosis-linked mutations in FUS/TLS. Ann. Neurol. 69: 152–162.

Kabashi, E., V. Bercier, A. Lissouba, M. Liao, E. Brustein *et al.*, 2011 FUS and TARDBP but not SOD1 interact in genetic models of amyotrophic lateral sclerosis. PLoS Genet. 7: e1002214.

Kino, Y., C. Washizu, E. Aquilanti, M. Okuno, M. Kurosawa *et al.*, 2011 Intracellular localization and splicing regulation of FUS/TLS are variably affected by amyotrophic lateral sclerosis-linked mutations. Nucleic Acids Res. 39: 2781–2798.

Kwiatkowski, Jr., T. J., D. A. Bosco, A. L. Leclerc, E. Tamrazian, C. R. Vanderburg *et al.*, 2009 Mutations in the FUS/TLS gene on chromosome 16 cause familial amyotrophic lateral sclerosis. Science 323: 1205–1208.

Lieber, M. R., 2010 The mechanism of double-strand DNA break repair by the nonhomologous DNA end-joining pathway. Annu. Rev. Biochem. 79: 181–211.

Liew, M., R. Pryor, R. Palais, C. Meadows, M. Erali *et al.*, 2004 Genotyping of single-nucleotide polymorphisms by high-resolution melting of small amplicons. Clin. Chem. 50: 1156–1164.

Meyer, M., M. H. de Angelis, W. Wurst, and R. Kuhn, 2010 Gene targeting by homologous recombination in mouse zygotes mediated by zinc-finger nucleases. Proc. Natl. Acad. Sci. USA 107: 15022–15026.

Miller, J. C., S. Tan, G. Qiao, K. A. Barlow, J. Wang *et al.*, 2011 A TALE nuclease architecture for efficient genome editing. Nat. Biotechnol. 29: 143–148.

Mori, K., S.-M. Weng, T. Arzberger, S. May, K. Rentzsch *et al.*, 2013 The C9orf72 GGGGCC repeat is translated into aggregating dipeptide-repeat proteins in FTLD/ALS. Science 339: 1335–1338.

Moscou, M. J., and A. J. Bogdanove, 2009 A simple cipher governs DNA recognition by TAL effectors. Science 326: 1501.
Porteus, M. H., and D. Carroll, 2005 Gene targeting using zinc finger nucleases. Nat. Biotechnol. 23: 967–973.
Qiu, Z., M. Liu, Z. Chen, Y. Shao, H. Pan *et al.*, 2013 High-efficiency and heritable gene targeting in mouse by transcription activator-like effector nucleases. Nucleic Acids Res. 41: e120.
Renton, A. E., E. Majounie, A. Waite, J. Simón-Sánchez, S. Rollinson *et al.*, 2011 A hexanucleotide repeat expansion in C9ORF72 is the cause of chromosome 9p21-linked ALS-FTD. Neuron 72: 257–268.
Reyon, D., S. Q. Tsai, C. Khayter, J. A. Foden, J. D. Sander *et al.*, 2012 FLASH assembly of TALENs for high-throughput genome editing. Nat. Biotechnol. 30: 460–465.
Rouet, P., F. Smih, and M. Jasin, 1994 Expression of a site-specific endonuclease stimulates homologous recombination in mammalian cells. Proc. Natl. Acad. Sci. USA 91: 6064–6068.
San Filippo, J., P. Sung, and H. Klein, 2008 Mechanism of eukaryotic homologous recombination. Annu. Rev. Biochem. 77: 229–257.
Sasayama, H., M. Shimamura, T. Tokuda, Y. Azuma, T. Yoshida *et al.*, 2012 Knockdown of the Drosophila fused in sarcoma (FUS) homologue causes deficient locomotive behavior and shortening of motoneuron terminal branches. PLoS ONE 7: e39483.
Sung, Y. H., I.-J. Baek, D. H. Kim, J. Jeon, J. Lee *et al.*, 2013 Knockout mice created by TALEN-mediated gene targeting. Nat. Biotechnol. 31: 23–24.
Taylor, J. P., 2013 Neuroscience. RNA that gets RAN in neurodegeneration. Science 339: 1282–1283.
Wefers, B., M. Meyer, S. Hensler, S. Panda, O. Ortiz *et al.*, 2012 Gene editing in one-cell embryos by zinc-finger and TAL nucleases. Curr. Protoc. Mouse Biol. 2: 347–364.
Wefers, B., M. Meyer, O. Ortiz, M. Hrabé de Angelis, J. Hansen *et al.*, 2013 Direct production of mouse disease models by embryo microinjection of TALENs and oligodeoxynucleotides. Proc. Natl. Acad. Sci. USA 110: 3782–3787.

*Communicating editor: D. Voytas*

GENETICS

**Supporting Information**
http://www.genetics.org/lookup/suppl/doi:10.1534/genetics.113.156570/-/DC1

# Highly Efficient Targeted Mutagenesis in Mice Using TALENs

**Sudeepta Kumar Panda, Benedikt Wefers, Oskar Ortiz, Thomas Floss, Bettina Schmid, Christian Haass, Wolfgang Wurst, and Ralf Kühn**


DOI: 10.1534/genetics.113.156570

**File S1**

**Supplementary methods**

**TALEN contruction and expression**

For the expression of TALENs in mammalian cells we used the expression vector pCAG-TALEN, that contains a CAG hybrid promoter region and a transcriptional unit comprising a sequence coding for the N-terminal amino acids 1 - 176 of TAL nuclease, located upstream of a pair of *Bsm*BI restriction sites, as described (17). This N-terminal regions includes an ATG start codon, a nuclear localisation sequence, a FLAG Tag sequence, a glycine rich linker sequence, a segment coding for 110 amino acids of the TAL protein AvrBs3 and the invariable N-terminal TAL repeat of the Hax3 TAL effector. Downstream of the central *Bsm*BI sites, the transcriptional unit contains 78 codons including an invariable C-terminal TAL repeat and 44 residues derived from the TAL protein AvrBs3, followed by the coding sequence of the FokI nuclease domain and a polyadenylation signal sequence. DNA segments coding for arrays of TAL repeats can be inserted into the *Bsm*BI sites of pCAG-TALEN in frame with the up- and downstream coding regions to enable the expression of predesigned TAL-Fok nuclease proteins. To derive TAL element DNA-binding domains we used the TAL effector motif (repeat) #11 of the Xanthomonas Hax3 protein (LTPEQVVAIAS**NI**GGKQALETVQRLLPVLCQAHG) to recognize A, the TAL effector motif #5 (LTPQQVVAIAS**HD**GGKQALETVQRLLPVLCQAHG) derived from the Hax3 protein to recognize C, and the TAL effector motif #4 (LTPQQVVAIAS**NG**GGKQALETVQRLLPVLCQAHG) from the *Xanthomonas* Hax4 protein to recognize T. To recognize a target G nucleotide we used the TAL effector motif #4 from the Hax4 protein with replacement of the amino acids 12 into N and 13 into N (LTPQQVVAIAS**NN**GGKQALETVQRLLPVLCQAHG). These elements were obtained by gene synthesis (Genscript, Piscataway, NJ, USA) and further amplified by PCR using primers that include BsaI sites outside of the coding region. For a 15 bp TALEN target sequence seven elements each are pooled in a pair of reactions together with *Bsa*I and T4 DNA ligase to create and ligate unique overhangs. Full length ligation products were recovered by gel extraction and inserted by seamless cloning (Gibson assembly, New England Biolabs) into pCAG-TALEN opened with *Bsm*BI. The integrity of all TALEN expression vectors was confirmed by DNA sequencing. The complete sequence of the vector encoded TALEN proteins is shown below [blue letters, nuclear localization sequence; red letters, FLAG tag; green letters, AvrBs3 N- and C-terminal sequences; black letters, TAL repeats (RVDs are underlined); orange letters, FokI nuclease domain; gray letters, linker sequences]:

**TALEN-Fus15A**

MGPKKKRKVAAADYKDDDDKPGGGGSGGGGVPASPAAQVDLRTLGYSQQQQEKIKPKVRSTVAQHHEALVGHGFTHAHIVALSQHPAALGTVA

VKYQDMIAALPEATHEAIVGVGKQWSGARALEALLTVAGELRGPPLQSGLDTGQLLKIAKRGGVTAVEAVHAWRNALTGAPLNLTPQQVVAIASH

DGGKQALETVQRLLPVLCQAHGLTPQQVVAIASNGGGKQALETVQRLLPVLCQAHGLTPQQVVAIASNGGGKQALETVQRLLPVLCQAHGLTPQ

QVVAIASNGGGKQALETVQRLLPVLCQAHGLTPQQVVAIASHDGGKQALETVQRLLPVLCQAHGLTPEQVVAIASNIGGKQALETVQRLLPVLCQA

HGLTPQQVVAIASNNGGKQALETVQRLLPVLCQAHGLTPQQVVAIASNNGGKQALETVQRLLPVLCQAHGLTPQQVVAIASNNGGKQALETVQR

LLPVLCQAHGLTPQQVVAIASNNGGKQALETVQRLLPVLCQAHGLTPQQVVAIASHDGGKQALETVQRLLPVLCQAHGLTPQQVVAIASNNGGKQ

ALETVQRLLPVLCQAHGLTPEQVVAIASNIGGKQALETVQRLLPVLCQAHGLTPQQVVAIASNNGGKQALETVQRLLPVLCQAHGLTPQQVVAIAS

HDGGRPALESIVAQLSRPDPALARSALTNDHLVALACLGGRPALDAVKKGLPHAPALIKRTNRRIPEGSDRLNQLVKSELEEKKSELRHKLKYVPHEYIE

LIEIARNSTQDRILEMKVMEFFMKVYGYRGKHLGGSRKPDGAIYTVGSPIDYGVIVDTKAYSGGYNLPIGQADEMQRYVEENQTRNKHINPNEWW

KVYPSSVTEFKFLFVSGHFKGNYKAQLTRLNHITNCNGAVLSVEELLIGGEMIKAGTLTLEEVRRKFNNGEINF

**TALEN-Fus15B**

MGPKKKRKVAAADYKDDDDKPGGGGSGGGGVPASPAAQVDLRTLGYSQQQQEKIKPKVRSTVAQHHEALVGHGFTHAHIVALSQHPAALGTVA

VKYQDMIAALPEATHEAIVGVGKQWSGARALEALLTVAGELRGPPLQSGLDTGQLLKIAKRGGVTAVEAVHAWRNALTGAPLNLTPEQVVAIASNI

GGKQALETVQRLLPVLCQAHGLTPEQVVAIASNIGGKQALETVQRLLPVLCQAHGLTPQQVVAIASNGGGKQALETVQRLLPVLCQAHGLTPEQVV

AIASNIGGKQALETVQRLLPVLCQAHGLTPQQVVAIASNGGGKQALETVQRLLPVLCQAHGLTPQQVVAIASNNGGKQALETVQRLLPVLCQAHGL

TPQQVVAIASNNGGKQALETVQRLLPVLCQAHGLTPQQVVAIASHDGGKQALETVQRLLPVLCQAHGLTPQQVVAIASHDGGKQALETVQRLLPV

LCQAHGLTPQQVVAIASNGGGKQALETVQRLLPVLCQAHGLTPQQVVAIASHDGGKQALETVQRLLPVLCQAHGLTPQQVVAIASNGGGKQALET

VQRLLPVLCQAHGLTPQQVVAIASHDGGKQALETVQRLLPVLCQAHGLTPQQVVAIASHDGGKQALETVQRLLPVLCQAHGLTPQQVVAIASHDG

GRPALESIVAQLSRPDPALARSALTNDHLVALACLGGRPALDAVKKGLPHAPALIKRTNRRIPEGSDRLNQLVKSELEEKKSELRHKLKYVPHEYIELIEIA

RNSTQDRILEMKVMEFFMKVYGYRGKHLGGSRKPDGAIYTVGSPIDYGVIVDTKAYSGGYNLPIGQADEMQRYVEENQTRNKHINPNEWWKVYP

SSVTEFKFLFVSGHFKGNYKAQLTRLNHITNCNGAVLSVEELLIGGEMIKAGTLTLEEVRRKFNNGEINF

**TALEN-Rik2A**

MGPKKKRKVAAADYKDDDDKPGGGGSGGGGVPASPAAQVDLRTLGYSQQQQEKIKPKVRSTVAQHHEALVGHGFTHAHIVALSQHPAALGTVA

VKYQDMIAALPEATHEAIVGVGKQWSGARALEALLTVAGELRGPPLQSGLDTGQLLKIAKRGGVTAVEAVHAWRNALTGAPLNLTPQQVVAIASN

NGGKQALETVQRLLPVLCQAHGLTPQQVVAIASNGGGKQALETVQRLLPVLCQAHGLTPQQVVAIASHDGGKQALETVQRLLPVLCQAHGLTPQ

QVVAIASNNGGKQALETVQRLLPVLCQAHGLTPEQVVAIASNIGGKQALETVQRLLPVLCQAHGLTPQQVVAIASHDGGKQALETVQRLLPVLCQA

HGLTPQQVVAIASNGGGKQALETVQRLLPVLCQAHGLTPEQVVAIASNIGGKQALETVQRLLPVLCQAHGLTPQQVVAIASNGGGKQALETVQRLL

PVLCQAHGLTPQQVVAIASHDGGKQALETVQRLLPVLCQAHGLTPQQVVAIASNGGGKQALETVQRLLPVLCQAHGLTPQQVVAIASNNGGKQA

LETVQRLLPVLCQAHGLTPQQVVAIASHDGGKQALETVQRLLPVLCQAHGLTPQQVVAIASHDGGKQALETVQRLLPVLCQAHGLTPQQVVAIASH

DGGRPALESIVAQLSRPDPALARSALTNDHLVALACLGGRPALDAVKKGLPHAPALIKRTNRRIPEGSDRLNQLVKSELEEKKSELRHKLKYVPHEYIELI

EIARNSTQDRILEMKVMEFFMKVYGYRGKHLGGSRKPDGAIYTVGSPIDYGVIVDTKAYSGGYNLPIGQADEMQRYVEENQTRNKHINPNEWWKV

YPSSVTEFKFLFVSGHFKGNYKAQLTRLNHITNCNGAVLSVEELLIGGEMIKAGTLTLEEVRRKFNNGEINF

**TALEN-Rik2B**

MGPKKKRKVAAADYKDDDDKPGGGGSGGGGVPASPAAQVDLRTLGYSQQQQEKIKPKVRSTVAQHHEALVGHGFTHAHIVALSQHPAALGTVA

VKYQDMIAALPEATHEAIVGVGKQWSGARALEALLTVAGELRGPPLQSGLDTGQLLKIAKRGGVTAVEAVHAWRNALTGAPLNLTPQQVVAIASH

DGGKQALETVQRLLPVLCQAHGLTPQQVVAIASNGGGKQALETVQRLLPVLCQAHGLTPQQVVAIASNNGGKQALETVQRLLPVLCQAHGLTPQ

QVVAIASNGGGKQALETVQRLLPVLCQAHGLTPQQVVAIASHDGGKQALETVQRLLPVLCQAHGLTPQQVVAIASNGGGKQALETVQRLLPVLCQ

AHGLTPQQVVAIASNGGGKQALETVQRLLPVLCQAHGLTPQQVVAIASNNGGKQALETVQRLLPVLCQAHGLTPQQVVAIASNNGGKQALETVQ

RLLPVLCQAHGLTPQQVVAIASHDGGKQALETVQRLLPVLCQAHGLTPEQVVAIASNIGGKQALETVQRLLPVLCQAHGLTPEQVVAIASNIGGKQA

LETVQRLLPVLCQAHGLTPQQVVAIASHDGGKQALETVQRLLPVLCQAHGLTPEQVVAIASNIGGKQALETVQRLLPVLCQAHGLTPQQVVAIASNK

GGRPALESIVAQLSRPDPALARSALTNDHLVALACLGGRPALDAVKKGLPHAPALIKRTNRRIPEGSDRLNQLVKSELEEKKSELRHKLKYVPHEYIELIE

IARNSTQDRILEMKVMEFFMKVYGYRGKHLGGSRKPDGAIYTVGSPIDYGVIVDTKAYSGGYNLPIGQADEMQRYVEENQTRNKHINPNEWWKVY

PSSVTEFKFLFVSGHFKGNYKAQLTRLNHITNCNGAVLSVEELLIGGEMIKAGTLTLEEVRRKFNNGEINF

**TALEN RVD arrays:**

| **TALEN** | **RVD sequence (w/o last half repeat)** |
|---|---|
| TALEN-Fus15A<br>Target sequence (5'-3') | **HD NG NG NG HD NI NN NN NN NN HD NN NI NN**<br>↓ ↓ ↓ ↓ ↓ ↓ ↓ ↓ ↓ ↓ ↓ ↓ ↓ ↓<br>**C T T T C A G G G G C G A G** |
| TALEN-Fus15B<br>Target sequence (5'-3') | **NI NI NG NI NG NN NN HD HD NG HD NG HD HD**<br>↓ ↓ ↓ ↓ ↓ ↓ ↓ ↓ ↓ ↓ ↓ ↓ ↓ ↓<br>**A A T A T G G C C T C T C C** |
| TALEN-Rik2A<br>Target sequence (5'-3') | **NN NG HD NN NI HD NG NI NG HD NG NN HD HD**<br>↓ ↓ ↓ ↓ ↓ ↓ ↓ ↓ ↓ ↓ ↓ ↓ ↓ ↓<br>**G T C G A C T A T C T G C C** |
| TALEN-Rik2B<br>Target sequence (5'-3') | **HD NG NN NG HD NG NG NN NN HD NI NI HD NI**<br>↓ ↓ ↓ ↓ ↓ ↓ ↓ ↓ ↓ ↓ ↓ ↓ ↓ ↓<br>**C T G T C T T G G C A A C A** |

**Construction of reporter plasmids**

Nuclease reporter plasmids were generated by the insertion of annealed sense and anti-sense oligonucleotides (Metabion, Martinsried, Germany), harboring the TALEN target sequences, (underlined) into the generic reporter plasmid pTAL-Rep, as described (17).

*Fus* target sense oligonucleotide:

5'-cggccaccatggtcgtctttcaggggcgagcacagacaggatcgcagggagaggccatattatg-3'

*Fus* target anti-sense oligonucleotide:

5'-cataatatggcctctccctgcgatcctgtctgtgctcgcccctgaaagacgaccatggtggc-3'

*C9orf72* target sense oligonucleotide:

5'-cgtgtcgactatctgccccccaccatctcctgctgttgccaagacaga-3'

*C9orf72* target anti-sense oligonucleotide:

5'-tctgtcttggcaacagcaggagatggtgggggcagatagtcgaca-3'

The integrity of all reporter plasmids was confirmed by DNA sequencing.

For the assessment of TALEN nuclease activities, expression vectors were cotransfected with the corresponding reporter plasmid into HEK 293 cells. Two days after transfection the cells were lysed and β-galactosidase was determined by chemiluminescense, as described (17).

**RNA isolation and cDNA synthesis**

Total RNA was isolated from tail tips using Trizol® (Life Technologies, Carlsbad, USA). Total RNA was reverse transcribed into cDNA using the Protoscript M-MuLV Taq-RT PCR kit (New England Biolabs) in presence of oligo $dT_{23}VN$, according to the manufacturer's protocol. Synthesized cDNA was diluted four times for further experiments.

**PCR amplification, cloning and sequencing**

Amplification of the diluted cDNA was performed by using Herculase II polymerase in 50 µl reactions with 30 cycles of {95 °C, 20 s; 51.5 °, 20 s; 72 °C, 30 s} using *Fus* specific primers (Table S3) to amplify 341 nucleotides spanning exon 14, exon 15 (which

encodes the NLS) and the 3'-UTR of the *Fus*, mRNA sequence. The resulting amplified product was subcloned using the StrataClone Blunt PCR Cloning Kit (Agilent, Waldbronn, Germany) and sequenced.

A hot start PCR protocol was employed for the amplification of genomic *Fus* gene fragments covering sequences 3.5kb upstream and 3.3 kb downstream of codon 513. PCR was carried out using Herculase II polymerase in 50 µl reactions with the 30 cycles of {95 °C, 20 s; 63 °, 20 s; 72 °C, 2 mins} using the gene specific primers (See Table S3: *Fus* 5' US and *Fus* 3' DS). PCR products were isolated by gel extraction (Qiagen, Hilden, Germany) and directly sequenced.

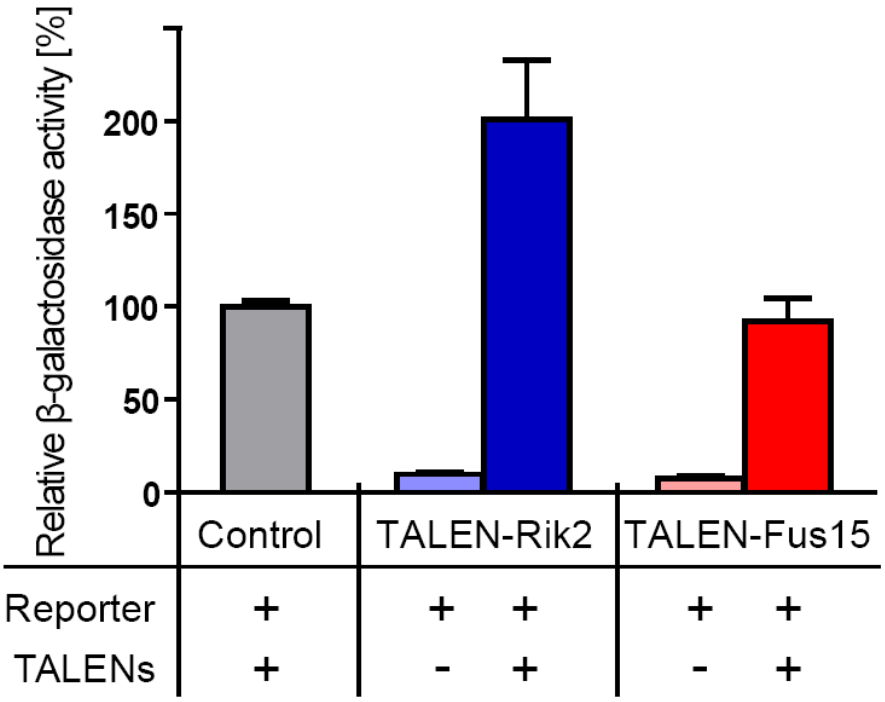


**Figure S1** TALEN activity in HEK 293 cells.

Cotransfection of reporter plasmids with TALEN-Rik2 or TALEN-Fus-15 vectors into HEK293 cells leads to nuclease dependent gene repair and β-galactosidase expression, as compared to the transfection of the reporter alone. Values are expressed as nuclease stimulated increase of β-galactosidase activity as compared to background levels without nuclease vectors (-) and to a TALEN/reporter standard (Control). The error bars represents s.d. in three replicates.

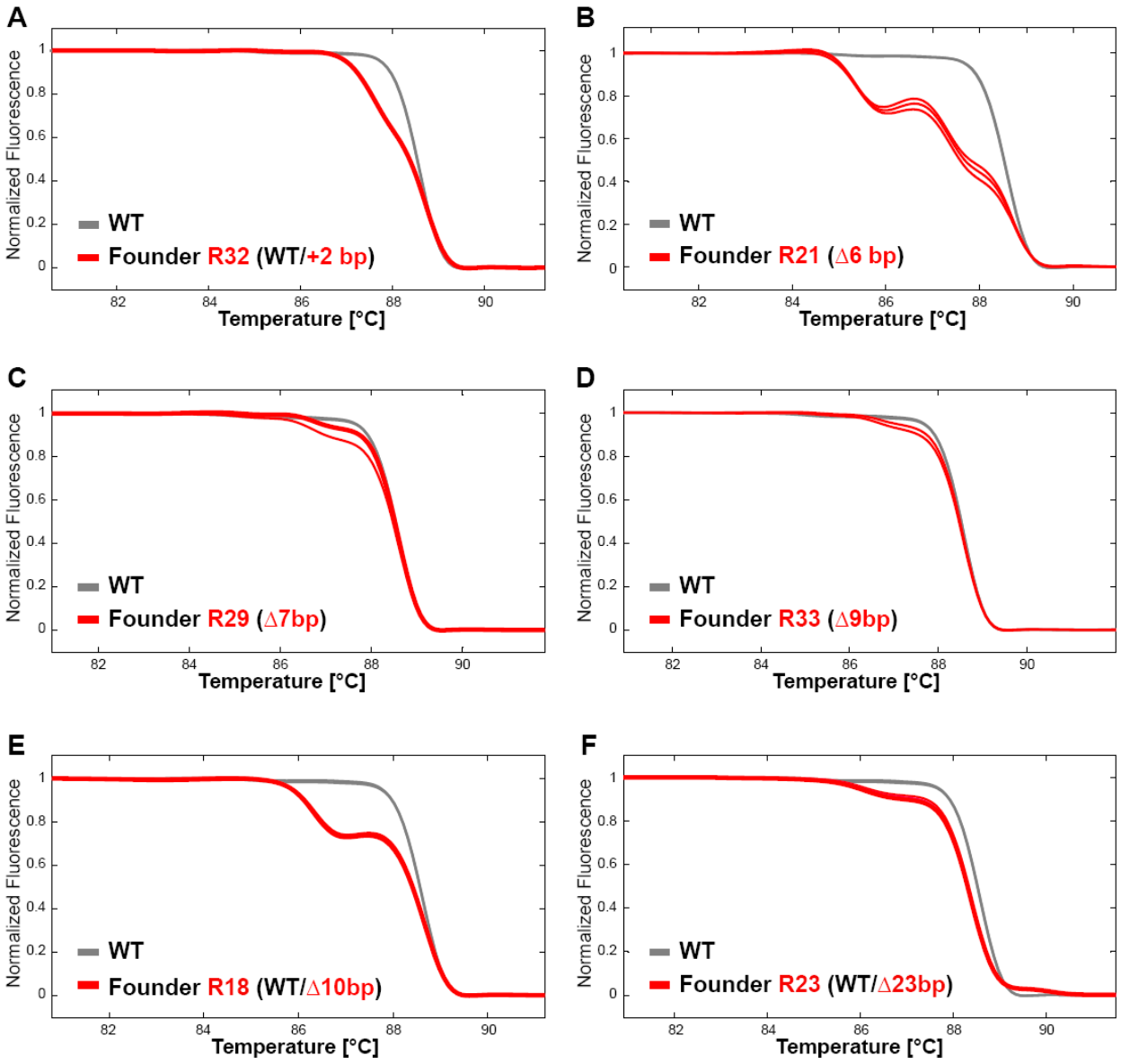


**Figure S2** HRMA for the identification of *C9orf72* founder mutants.

Melting analysis of PCR products amplified in triplicate from tail DNA of founder R32 **(A)**, R21 **(B)**, R29 **(C)**, R33 **(D)**, R18 **(E)**, and R23 **(F)** (red curves, overlayed) or from a wildtype control mouse (grey curves, overlayed) demonstrated the presence of mutant allele(s). The genotype of mutant alleles is indicated in parentheses; see Figure 3 for the allele sequences.

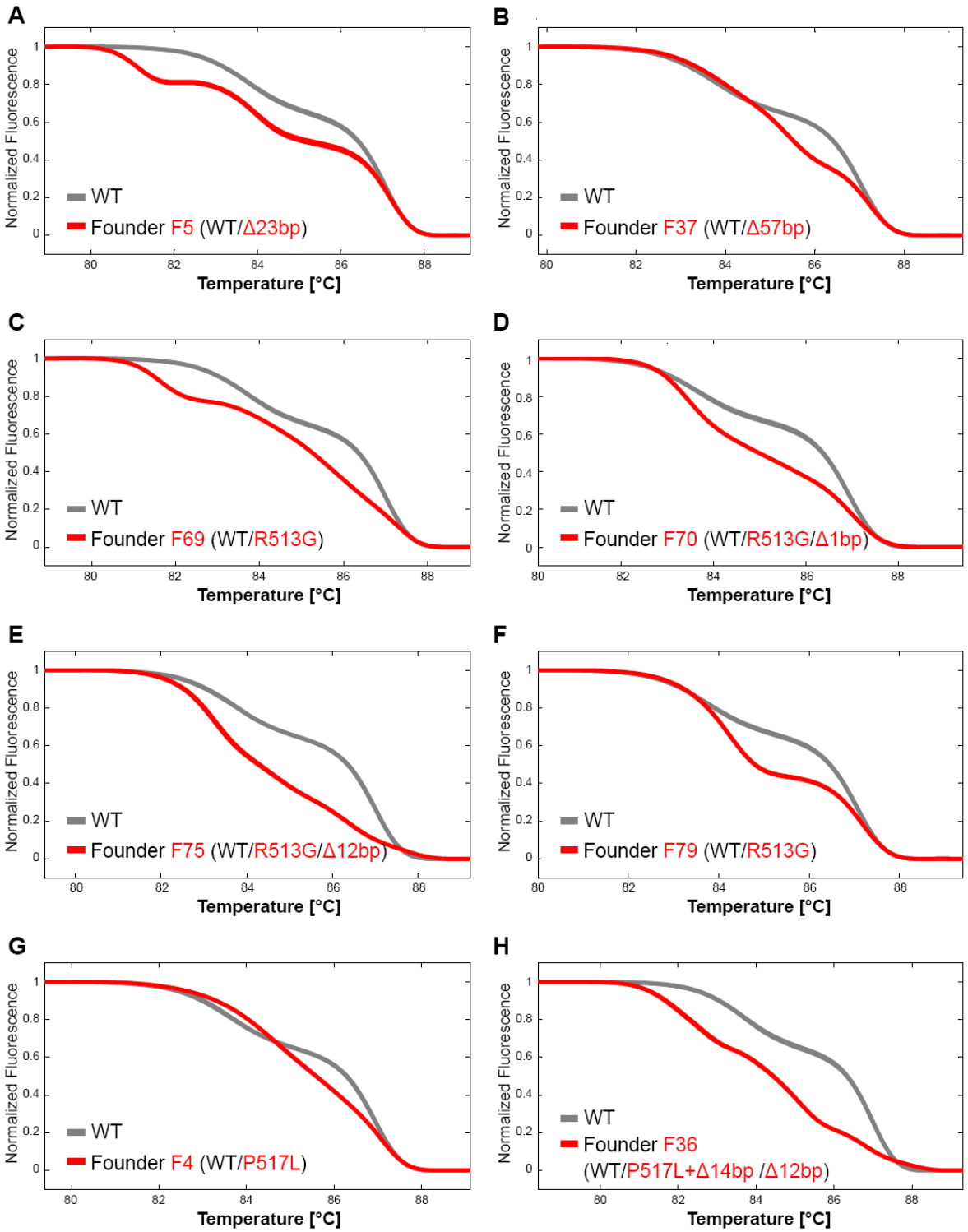


**Figure S3** HRMA for the identification of *Fus* founder mutants.
Melting analysis analysis of PCR products amplified in triplicate from tail DNA of founder F5 **(A)**, F37 **(B)**, F69 **(C)**, F70 **(D)**, F75 **(E)**, and F79 **(F)** using TALEN-Fus15 and ODN$^{R513G}$ and of founder F4 **(G)**, and F36 **(H)** using TALEN-Fus15 and ODN$^{P517L}$ (red curves, overlayed), or from a wildtype control mouse (grey curves, overlayed). The genotype of mutant alleles is indicated in parentheses; see Figure 4 for the allele sequences.

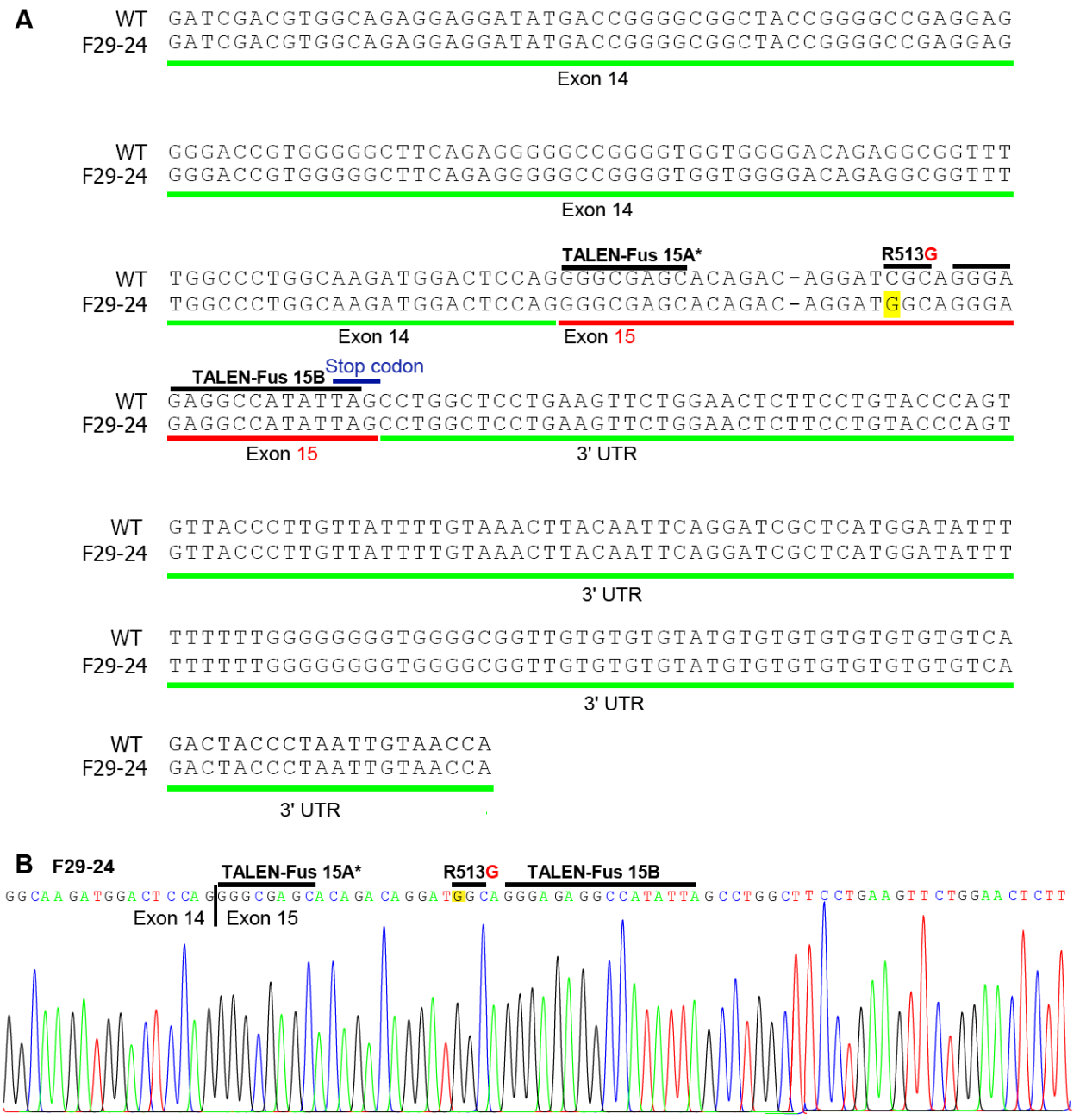


**Figure S4** Sequence analysis of *Fus*$^{R513G}$ cDNA.
**(A)** Sequence comparison of the cloned PCR product representing 341 bp of the *Fus* cDNA sequence, including exon 14, exon 15 and 3´UTR sequences, derived from the mutant pup F29-24 in comparison to wildtype cDNA sequence. **(B)** Chromatogram showing the sequencing peaks of the cloned PCR product covering the *Fus* codon 513 (nucleotide replacement highlighted in yellow). The positions of exon 14, exon 15, exon boundary, stop codon, 3' UTR, TALEN binding sites and of the R513G replacement are indicated.

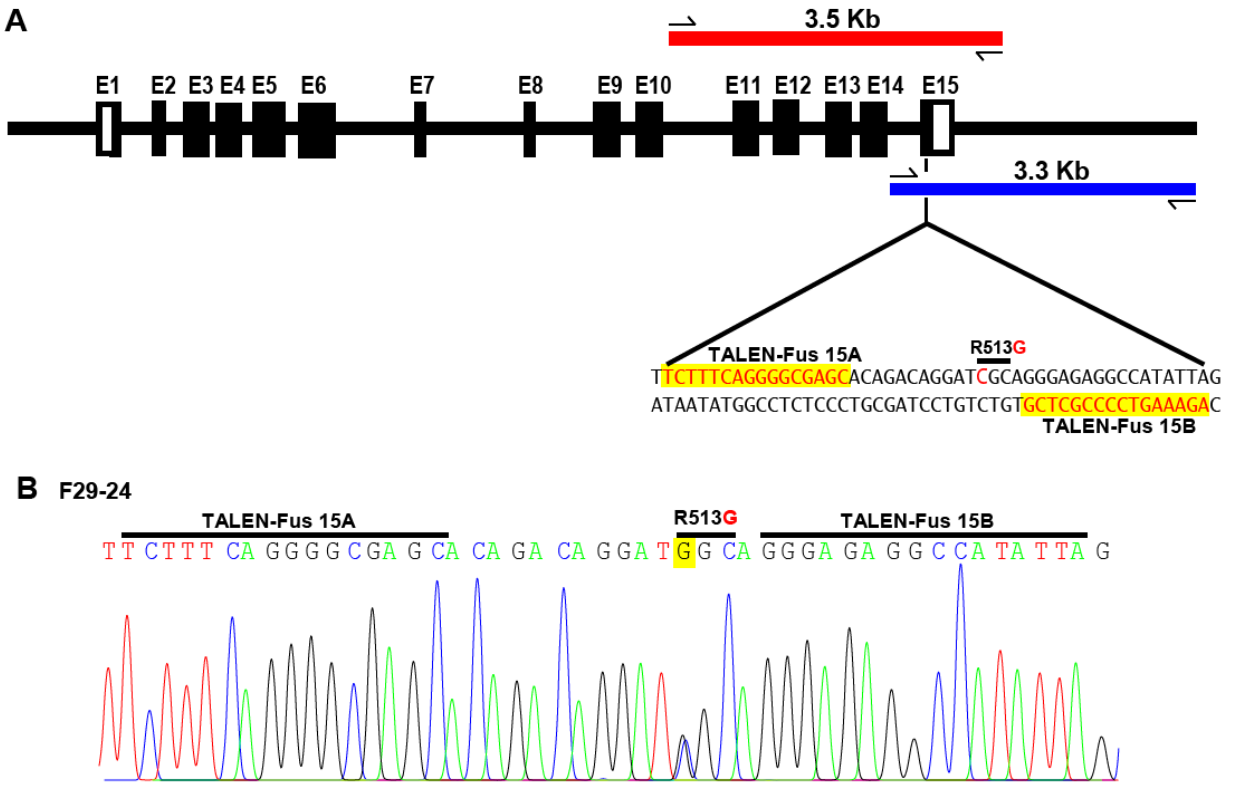


**Figure S5** Sequence analysis of the *Fus*$^{R513G}$ locus.
**(A)** Schematic drawing of the mouse *Fus* gene, showing the PCR amplified segments of 3.5 kb and 3.3 kb PCR product, which both overlap codon 513. Amplification was performed using tail DNA of the heterozygous (*Fus*$^{R513G}$) pup F29-24 such that equal amounts of PCR products are derived from the *Fus* wildtype and the *Fus*$^{R513G}$ alleles are expected. **(B)** Chromatogram covering the sequence around codon 513, showing a mixed peak at the position of the targeted *Fus*$^{R513G}$ nucleotide replacement.


**Figure S6** Nucleotide polymorphisms in TALEN-Fus15 off-target sites 1 and 3.
Sequencing of HRMA PCR products revealed single nucleotide polymorphisms between wildtype C57BL/6 controls and mutant founder animals in the TALEN-Fus15 off-site 1 (**A**) and off-site 3 (**B**). These polymorphisms were identified as strain polymorphisms, resulting from the mixed genetic backgrounds (C57BL/6, DBA/2, and FVB/N) of founders. Predicted TALEN off-target binding sites and HRMA primer binding sites are indicated.

**Table S1 Germline transmission of TALEN-induced mutations**

| Microinjection experiment | Founder | Pups | Mutant pups |
|---|---|---|---|
| TALEN-Rik2 | R23 | 15 | 7 |
| TALEN-Fus15 + ODN$^{R513G}$ | F5 | 10 | 1 |
| | F18 | 23 | 13 |
| | F29 | 15 | 8 |
| | F37 | 17 | 8 |
| | F70 | 3 | 2 |
| | F75 | 7 | 4 |
| TALEN-Fus15 + ODN$^{P517L}$ | F36 | 12 | 8 |

**Table S2 Potential off-target sites of TALEN-Rik2 and TALEN-Fus15.**

| Locus | Chromosomal position | Target sequence A (5′-3′) | Spacer length | Target sequence B (5′-3′) | Dimer type |
|---|---|---|---|---|---|
| ***C9orf72*** | ***Chr4:35218811-35218854*** | **T CTGTCTTGGCAACAG** | **14** | **T GTCGACTATCTGCCC** | A-B |
| *Csmd1* | *Chr8:16813743-16813785* | **T CTAACTTGACAACAA** | **13** | **T CTATCTAATTAACAA** | A-A |
| Intergenic | *Chr8:34491313-34491356* | **T CTGTCTTCCCACCAG** | **14** | **T ATCAACTACATAACC** | A-B |
| *Gfra1* | *Chr19:58314874-58314920* | **T CTGTGTTCACAAAAG** | **17** | **T CTGTCCTGACCACAG** | A-A |
| Intergenic | *Chr9:112015226-112015268* | **T CTGCCTTGACAACCT** | **13** | **T TTCAACTATGTGCCC** | A-B |
| Intergenic | *Chr19:4408724-4408766* | **T CAGCCTTGGCAACAT** | **13** | **T CTCTCTTCCCAAAAG** | A-A |
| ***Fus*** | ***Chr7:127981783-127981827*** | **T CTTTCAGGGGCGAGC** | **15** | **T AATATGGCCTCTCCC** | A-B |
| Intergenic | *Chr4:149785023-149785065* | **T CATTCAAGCCGAAGC** | **13** | **T AATATGACATCTCCC** | A-B |
| *Zdhhc5* | *Chr2:84705308-84705354* | **T CTATCAAAGGCAACC** | **17** | **T AAGATGACCACTCCA** | A-B |
| *Sec23b* | *Chr2:144575630-144575674* | **T CTTTACAGAACTAAC** | **15** | **T AAAATGACCTCCCCC** | A-B |
| *AC122296.2-201* | *Chr6:67120279-67120328* | **T CTTCCACAACCAAGC** | **20** | **T CTTTCCGGCCCAAGC** | A-A |
| Intergenic | *ChrX:35868551-35868598* | **T CTTACAAAGCCAAAC** | **18** | **T CATATAACTTCTCCA** | A-B |

TALEN-Rik2 and TALEN-Fus15 binding sequences are shown in bold letters. Nucleotides of off-target sites matching the target are shown in black, mismatches in off-target sites are shown in red. A-B: heterodimeric target sequence, A-A: homodimeric target sequence.

**Table S3 Oligonucleotides used in this study**

| Amplicon Name | Forward Primer (5'-3') | Reverse Primer (5'-3') |
|---|---|---|
| *Fus* | CTATGGAGATGATCGACGTG | TGGTTACAATTAGGGTAGTCTG |
| *Fus* HRMA | CATGGGTAGGGTAGTTCAGTAACACGT | ACACTGGGTACAGGAAGAGTTCCAG |
| *Fus* OS1 | CCAACCACCCATGGCTTCTTATTA | GCACTGGGGTAGCATACACACATC |
| *Fus* OS2 | GCTTTCCTTGTTTTAGCACTCTGC | CTGCAGCCACTCCCTAAACTTCTT |
| *Fus* OS3 | CTCCCTTCCCTCTGTCTGTCTCTG | TTTCTGGGTTACCTGGGGTCAGTA |
| *Fus* OS4 | CCCAAGCAGCTGGACTAAGGATCT | ACACCTGGTGGTAGTTCATTGCTT |
| *Fus* OS5 | GTGAGTTCAAGTCCAGCCCAGTCT | GCTTTGTGGCAGGCACTTTTATTC |
| *Fus* R513G | TGGGTAGGGTAGTTCAGTAAC | ACAAGGGTAACACTGGGTAC |
| *Fus* 5' US | GTCATCAAGCACCTTTACCTG | TGGTTACAATTAGGGTAGTCTG |
| *Fus* 3' DS | TGGGTAGGGTAGTTCAGTAAC | ACTCTTGTCTAGCAGTGATTCTC |
| *Rik* | TTAGCTGAAATGGTTTGGAGAC | CATCACTGAGAAGCACTTGG |
| *Rik* HRMA | CGTTCGGATAATGTGAGACCTG | CAAAGGTAGCCGCCAACAAG |
| *Rik* OS1 | TGACTGACAGGCTTCACAGAGAGC | CTACTGGGGACTGATGACTACCTG |
| *Rik* OS2 | CACAGGGACTTTGTGTGCACTCTT | AAACCAGAGCATGGCTTTGAAAAA |
| *Rik* OS3 | GAAGATAAACAGGAGCCGCATGAA | TGACTCACTAAGGGCCATTCCTTC |
| *Rik* OS4 | TACAGGCTTCACTCTGTGGGGTTT | CCAGATCTGACTCAGGTAATGTGA |
| *Rik* OS5 | AGTGGCCCCACACAGAAGAGTAAG | AGGAATGTGTGGGCAAATCTTGTT |
| **Sequencing Primer** | | |
| *Fus* 5´RI 3 | — | GCACACCCTTCAAGTCTCTG |
| *Fus* 5´RI 2 | GCGGGAGTGGGTGGGTTTTTG | — |
| *Fus* 3´RI 5 | GACAATTTTCCCGAAATGGGC | — |